IRIS AperTO

UNIVERSITÀ DEGLI STUDI DI TORINO

AperTO - Archivio Istituzionale Open Access dell'Università di Torino

Structural and photophysical evaluation of O-alkoxy substituted BODIPY dyes in liposomes

This is a pre print version of the following article:

Original Citation:

Availability:

This version is available http://hdl.handle.net/2318/2155491 since 2026-08-14T09:50:34Z

Published version:

DOI:10.1039/D6OB00623J

Terms of use:

Open Access

Anyone can freely access the full text of works made available as "Open Access". Works made available under a Creative Commons license can be used according to the terms and conditions of said license. Use of all other works requires consent of the right holder (author or publisher) if not exempted from copyright protection by the applicable law.

(Article begins on next page)

08 November 2026

Organic & Biomolecular Chemistry

Accepted Manuscript

Published on 05 August 2026

Licensed under CC-BY 4.0

Check for updates

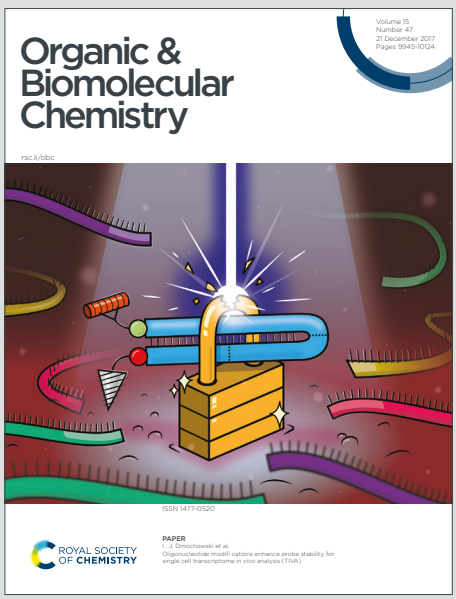

This is an Accepted Manuscript, which has been through the Royal Society of Chemistry peer review process and has been accepted for publication.

Accepted Manuscripts are published online shortly after acceptance, before technical editing, formatting and proof reading. Using this free service, authors can make their results available to the community, in citable form, before we publish the edited article. We will replace this Accepted Manuscript with the edited and formatted Advance Article as soon as it is available.

You can find more information about Accepted Manuscripts in the Information for Authors.

Please note that technical editing may introduce minor changes to the text and/or graphics, which may alter content. The journal's standard Terms & Conditions and the Ethical guidelines still apply. In no event shall the Royal Society of Chemistry be held responsible for any errors or omissions in this Accepted Manuscript or any consequences arising from the use of any information it contains.

Organic & Biomolecular Chemistry Accepted Manuscript

ARTICLE

Structural and photophysical evaluation of O-alkoxy substituted BODIPY dyes in liposomes

Received 00th January 20xx,
Accepted 00th January 20xx

DOI: 10.1039/x0xx00000x

Martina Fresia,[a]† Francesco Marra,[a]† Giacomo Renno,[a,b] Giada Fregnan,[c] Davide Zanetti,[a] Federica Micheletto,[a] Paolo Ettore Porporato,[c] Francesca Cardano,[a,d]* Marco Blangetti,[a]* Andrea Fin[a,d]*

Bright and easy to synthesize probes for bioimaging read-outs are constantly required to visualize and deeply understand biochemical structures and functionalities. Hence, the visualization of cellular membranes is key due to their biological role. In this work, six rationally designed alkoxy-substituted 4,4-difluoro-4-bora-3a,4a-diaza-*s*-indacene (BODIPY) fluorophores have been synthesized and investigated. This design aims to evaluate how the presence of structurally different short ethylene glycol subunits in *para*-position of *meso*-phenyl substituted BODIPY impacts on the overall molecular hydrophilic/hydrophobic balance, on the related optical properties and on the staining of lipid bilayer membranes in large unilamellar vesicles (LUVs) as cell membrane models. The photophysical properties have been deeply studied with respect to the probe structure obtaining versatile key data to support the design of new fluorescent sensors for biological applications.

Introduction

Visualizing cellular and subcellular compartments by minimally invasive techniques with high spatial and temporal resolution remains today a significant challenge in chemical biology. Bioimaging has proven highly effective in delivering biochemical information, enabling precise visualization and understanding of biomolecular events and structures useful for investigating physiological and pathological states.[1–5] Membrane bilayers play essential roles by defining intracellular composition as well as by regulating dynamic processes.[6] Biological membranes exhibit a complex organization, composed of diverse lipid bilayers and associated proteins that contribute structurally and functionally to cross-membrane transport and various biochemical activities.[7] Among the various fluorescent probes available, emissive small molecules are considered first choice candidates for membrane imaging.[8–13] They are highly versatile in terms of synthetic accessibility and they are optimal substrates for synthetic modifications. Small fluorescent dyes are usually denoted by diversified optical properties, and generally favourable biocompatibility.[1,4,5] Their design typically focuses on hydro/lipophilic balanced structures, enabling selective membrane staining for an effective targeted imaging. Over the years, numerous families of fluorescent probes have been explored for membrane staining, each featuring distinct molecular scaffolds, peculiar photophysical traits, and sensitivity to environmental factors.[8–18] Nonetheless, a strong demand of novel dyes with enhanced optical performances and improved specificity for biological compartments is remaining. In this context, 4,4-difluoro-4-bora-3a,4a-diaza-*s*-indacene fluorophores, commonly known as BODIPY dyes, are today recognised as one of the more versatile and used fluorophore in many research and applicational fields.[19–21] Since their discovery in 1968, this class of dyes has been deeply investigated in different areas owing to the current incremented commercial availability of key building blocks as well as of final probes: those include materials science, chemical biology, and biomedical diagnostic, among others.[22–25] Their synthetic feasibility, together with the easiness of chemical and structural modification, denotes an interesting class of functional fluorophores. BODIPYs are characterized by optimal photophysical properties including good photo- and thermal stability, narrow absorption and emission peaks in the visible region of the spectrum and beyond, negligible triplet-state formation accompanied by high fluorescence quantum yields and large molar absorption coefficients which brings to significant brightness.[26–28] Their current research interest in chemical biology strictly relates to super resolution imaging outcomes, organelle targeting, bio-chemo sensing, fluorescence photoactivation and mapping of intrinsic biological properties such as biological viscosity due to their molecular rotor nature.[29–35] In this work, we rationally designed a small library of *meso*-substituted BODIPY dyes to introduce two or three oxyethylene subunits on the *para*-position of a *meso*-phenyl substituent approaching a PEGylation strategy. Two different terminals (MeO–compounds: **1-3** and *n*-BuO–compounds: **4-6**) have been considered to evaluate the overall

[a] Department of Chemistry, University of Torino, Via P. Giuria 7, 10125 Torino, Italy
[b] Department of Organic Chemistry, University of Geneva, 30 quai Ernest Ansermet, 1211 Geneva, Switzerland
[c] Department of Molecular Biotechnology and Health Sciences, Molecular Biotechnology Center "Guido Tarone", University of Torino, Via Nizza 52, 10126 Torino, Italy
[d] Center for Sustainable Future Technologies (CSFT), Istituto Italiano di Tecnologia (IIT), Via Livorno 60, 10144, Torino, Italy
† These authors contributed equally.

structural properties in terms of tuned hydro/lipophilic balance for targeting biological membranes (Figure 1a). The rational design for the BODIPYs' library herein reported aimed at understanding the structure to function effect, without perturbing the photophysical features of the fluorophore, derived by modulating the hydrophilic/hydrophobic character at the BODIPY *meso* position by varying the length of ethylene glycol chains and the terminal alkyl moieties. While keeping a compact probe structure the insertion of one, two or three ethylene glycol subunits is here proposed to compensate for the lipophilic BODIPY conferring an amphiphilic character to the final dyes and therefore promoting the interaction with biological membranes. The variation of the terminal alkyl moieties instead is here proposed to compensate the hydrophilicity of the glycol bridge and fine tune the solubility features in hydrophobic media. The synthesized compounds have been investigated in their photophysical properties in organic solvents and in aqueous buffer solution to completely understand the photophysical response and, lately, to evaluate their partition kinetics into large unilamellar vesicles (LUVs) as lipid bilayer membrane models. The best performing dyes of the synthetised library of BODIPYs were finally tested in cell imaging. This approach, previously reported by our research groups for investigating squaraine and core-substituted naphthalenediimides (cNDIs) fluorophores, allows to correlate the effects of modified hydro/lipophilic molecular structure to the optical traits in the LUVs interaction, furnishing a complete and detailed dataset for improving the design possibilities within the BODIPY fluorophores family toward chemical biology applications.[9,10]

Material and methods

All reactions involving air-sensitive reagents were performed under nitrogen in oven-dried glassware using the syringe septum cap technique. Anhydrous dichloromethane (DCM) was distilled under nitrogen over CaH_2 prior to use. Anhydrous tetrahydrofuran (THF) was distilled under nitrogen over Na/benzophenone ketyl prior to use. Unless specified, all reagents were purchased from common suppliers and used as received. Reactions were monitored by thin-layer chromatography (TLC) carried out on 0.25 mm silica gel coated aluminium plates (60 Merck F254) with UV light (254 nm) as visualizing agent. Chromatographic separations were carried out under pressure on silica gel (40–63 μm, 230–400 mesh) using flash-column techniques. Alkoxylated (4-(2-(2-Methoxyethoxy)ethoxy)-, (4-(2-(2-(2-methoxyethoxy)ethoxy)ethoxy)-, (4-(2-(2-butoxyethoxy)ethoxy)-, and (4-(2-(2-(2-butoxyethoxy)ethoxy)ethoxy)- benzaldehydes have been synthesized according to the known literature procedure.[24,36–39] Full characterisation data, including copies of ^{1}H and ^{13}C NMR spectra (Supplementary Information), have been reported for both the newly synthesized and the known compounds.

Instrumentation

^{1}H NMR (600 MHz), ^{13}C{^{1}H} (150 MHz) NMR spectra were recorded on a Jeol ECZR600 spectrometer at room temperature using residual solvent peak as an internal reference. Chemical shifts (δ) are given in parts per million (ppm) and coupling constants (*J*) in Hertz (Hz). Multiplicities are reported as follows: s (singlet), d (doublet), t (triplet), q (quartet), quint (quintet), sext (sextet), hept (septet), m (multiplet), br (broad). HRMS analyses was performed using an Orbitrap IQ-X mass spectrometer (Thermo Fisher Scientific) equipped with a Heated ElectroSpray Ionization (HESI) source. DLS measurements were performed on Malvern Zetasizer Nano ZS instrument (Malvern Panalytical Ltd, UK).

Synthesis

General procedure for the synthesis of BODIPY dyes 1-6.

The reactions were performed under an inert atmosphere (nitrogen). To a stirred solution of the appropriate aldehyde (3.0 mmol) and 2,4-dimethylpyrrole (0.62 mL, 6 mmol, 2.0 eq.) in anhydrous DCM (30 mL, 0.1 M), a catalytic amount of TFA (5 drops) was added, and the reaction mixture was stirred at room temperature (rt) until complete consumption of the aldehyde, as monitored by TLC analysis (12 h). DDQ (681 mg, 3.0 mmol, 1.0 eq.) was subsequently added, and the resulting mixture was stirred at room temperature. After 3 h, the mixture was washed with H_2O, the organic layer was dried over anhydrous Na_2SO_4 and concentrated under reduced pressure. The residue was dissolved in anhydrous DCM (20 mL, 0.15 M), and *N*,*N*-diisopropylethylamine (DIPEA, 5.20 mL, 30.0 mmol, 10.0 eq.) was added at 0 °C. The mixture was stirred for 10 min and then $BF_3{\cdot}OEt_2$ (24.0 mmol, 8.0 eq.) was slowly added. The resulting mixture was stirred at room temperature overnight. The reaction mixture was concentrated under reduced pressure, and the crude product was purified by flash column chromatography on silica gel.

***Meso*-(4-methoxyphenyl)-1,3,5,7-tetramethyl BODIPY (1):** As in the general procedure, starting from 4-anisaldehyde. Purification by flash column chromatography on silica gel (petroleum ether/EtOAc 9/1 v/v, R_f = 0.38) gave **1** as a red solid (276 mg, 26%). ^{1}H NMR (600 MHz, $CDCl_3$) δ 7.17 (d, *J* = 8.6 Hz, 2H), 7.01 (d, *J* = 8.6 Hz, 2H), 5.97 (s, 1H), 3.87 (s, 3H), 2.55 (s, 3H), 1.43 (s, 3H). ^{13}C{1H} NMR (150 MHz, $CDCl_3$) δ 160.3, 155.4, 143.3, 142.0, 132.0, 129.4, 127.2, 121.2, 114.7, 55.5, 14.7. All the experimental data are in good accordance with those reported in the literature.[40]

***Meso*-(4-(2-(2-methoxyethoxy)ethoxy)phenyl)-1,3,5,7-tetramethyl BODIPY (2):** As in the general procedure, starting from (4-(2-(2-methoxyethoxy)ethoxy)benzaldehyde. Purification by flash column chromatography on silica gel (petroleum ether/EtOAc 7/3 v/v, R_f = 0.23) gave **2** as a red solid (117 mg, 10%). ^{1}H NMR (600 MHz, $CDCl_3$) δ 7.14 (d, *J* = 8.7 Hz, 2H), 7.01 (d, *J* = 8.7 Hz, 2H), 5.96 (s, 2H), 4.27 – 4.11 (m, 2H), 3.90 (ddd, *J* = 5.8, 3.5, 0.9 Hz, 2H), 3.82 – 3.69 (m, 2H), 3.60 (ddd, *J* = 5.8, 3.5, 0.9 Hz, 2H), 3.40 (s, 3H), 2.54 (s, 3H), 1.41 (s, 3H). ^{13}C{^{1}H} NMR (150 MHz, $CDCl_3$) δ 159.5, 155.4, 143.3, 141.9, 131.9, 129.3, 127.3, 121.2, 115.3, 72.1, 71.0, 69.9, 67.6, 59.2, 14.7, 14.7. All the experimental data are in good accordance with those reported in the literature.[41]

***Meso*-(4-(2-(2-(2-methoxyethoxy)ethoxy)ethoxy)phenyl)-1,3,5,7-tetramethyl BODIPY (3):** As in the general procedure, starting from 4-(2-(2-(2-methoxyethoxy)ethoxy)ethoxy)benzaldehyde.

Organic & Biomolecular Chemistry Accepted Manuscript

This journal is © The Royal Society of Chemistry 20xx

Please do not adjust margins

Purification by flash column chromatography on silica gel (petroleum ether/DCM 6/4 v/v, R_f = 0.40) gave **3** as a bright orange solid (356 mg, 24%). ^{1}H NMR (600 MHz, $CDCl_3$) δ 7.15 (d, *J* = 8.7 Hz, 2H), 7.02 (d, *J* = 8.7 Hz, 2H), 5.97 (s, 2H), 4.18 (m, 2H), 3.93 – 3.90 (m, 2H), 3.77 (dd, *J* = 5.9, 3.7 Hz, 2H), 3.71 (dd, *J* = 5.9, 3.7 Hz, 2H), 3.69 – 3.65 (m, 2H), 3.60 – 3.55 (m, 2H), 3.39 (s, 3H), 2.55 (s, 6H), 1.42 (s, 6H). ^{13}C{^{1}H} NMR (150 MHz, $CDCl_3$) δ 159.5, 155.4, 143.3, 141.9, 132.0, 129.3, 127.4, 121.2, 115.3, 721, 71.0, 70.8, 70.7, 69.9, 67.6, 59.2, 14.7, 14.7. HRMS (ESI): m/z calcd for $C_{26}H_{33}BF_2N_2O_4$ + Na^+: 509.2394 $[M+Na]^+$; found: 509.2411. All the experimental data are in good accordance with those reported in the literature.[42]

***Meso*-(4-butoxyphenyl)-1,3,5,7-tetramethyl BODIPY (4):** As in the general procedure, starting from 4-butoxybenzaldehyde. Purification by flash column chromatography on silica gel (petroleum ether/DCM 1/1 v/v, R_f = 0.33) gave **4** as a red solid (332 mg, 28%). ^{1}H NMR (600 MHz, $CDCl_3$) δ 7.15 (d, *J* = 8.6 Hz, 2H), 6.99 (d, *J* = 8.6 Hz, 2H), 5.97 (s, 2H), 4.01 (t, *J* = 6.6 Hz, 2H), 2.55 (s, 6H), 1.81 (quint, *J* = 6.6 Hz, 2H), 1.53 (sext, *J* = 7.4 Hz, 2H), 1.01 (t, *J* = 7.4 Hz, 3H). ^{13}C{^{1}H} NMR (150 MHz, $CDCl_3$) δ 159.9, 155.3, 143.3, 142.2, 132.0, 129.3, 126.9, 121.2, 115.2, 67.9, 31.4, 19.4, 14.7, 14.1. HRMS (ESI): m/z calcd for $C_{23}H_{27}BF_2N_2O$ + H^+: 397.2257 $[M+H]^+$; found: 397.2272.

***Meso*-(4-(2-(2-butoxyethoxy)ethoxy)phenyl)-1,3,5,7-tetramethyl BODIPY (5):** As in the general procedure, starting from (4-(2-(2-butoxyethoxy)ethoxy)benzaldehyde. Purification by flash column chromatography on silica gel (petroleum ether/Et_2O 7/3 v/v, R_f = 0.30) gave **5** as a red solid (100 mg, 15%). ^{1}H NMR (600 MHz, $CDCl_3$) δ 7.15 (d, *J* = 8.6 Hz, 2H), 7.02 (d, *J* = 8.6 Hz, 2H), 5.97 (s, 2H), 4.22 – 4.14 (m, 2H), 3.93 – 3.87 (m, 2H), 3.77 – 3.73 (m, 2H), 3.66 – 3.60 (m, 2H), 3.48 (t, *J* = 6.8 Hz, 2H), 2.54 (s, 6H), 1.58 (quint, *J* = 6.8 Hz, 2H), 1.42 (s, 6H), 1.37 (sext, *J* = 7.4 Hz, 2H), 0.92 (t, *J* = 7.4 Hz, 3H). ^{13}C{^{1}H} NMR (150 MHz, $CDCl_3$) δ 159.5, 155.4, 143.3, 142.0, 132.0, 129.3, 127.3, 121.2, 115.3, 71.4, 71.1, 70.3, 69.9, 67.7, 31.8, 19.4, 14.7, 14.7, 14.1. HRMS (ESI): m/z calcd for $C_{27}H_{35}BF_2N_2O_3$ + H^+: 485.2786 $[M+H]^+$; found: 485.2782.

***Meso*-(4-(2-(2-(2-butoxyethoxy)ethoxy)ethoxy)phenyl)-1,3,5,7-tetramethyl BODIPY (6):** As in the general procedure, starting from (4-(2-(2-(2-butoxyethoxy)ethoxy)ethoxy)benzaldehyde. Purification by flash column chromatography on silica gel (petroleum ether/Et_2O 1/1 v/v, R_f = 0.27) gave **6** as a bright orange semisolid (218 mg, 18%). All the experimental data have been previously reported by us and listed herein for completeness.[24] ^{1}H NMR (600 MHz, $CDCl_3$): δ 7.10 (d, *J* = 8.7 Hz, 2H), 6.97 (d, *J* = 8.7 Hz, 2H), 5.93 (s, 2H), 4.26-4.22 (m, 2H), 3.93-3.90 (m, 2H), 3.77-3.74 (m, 2H), 3.73-3.70 (m, 2H), 3.69-3.65 (m, 2H), 3.61-3.58 (m, 2H), 3.43 (t, *J* = 6.7 Hz, 2H), 2.49 (s, 6H), 1.56-1.51 (m, 2H), 1.37 (s, 6H), 1.34-1.30 (m, 2H), 0.87 (t, *J* = 7.4 Hz, 3H). ^{13}C {^{1}H} NMR (150 MHz, $CDCl_3$): δ 159.5, 155.4, 143.3, 141.9, 131.9, 129.3, 127.3, 121.2, 115.3, 71.3, 71.0, 70.8, 70.8, 70.2, 69.8, 67.6, 31.8, 19.4, 14.7, 14.7, 14.0.

Photophysical assays

Solvents used for the spectroscopy measurement were purchased from Sigma Aldrich and TCI. Aqueous buffer solutions were prepared with de-ionized water (Millipore RiOs 3 Water System), sodium phosphate monobasic monohydrate, disodium hydrogen phosphate dihydrate and sodium chloride (Biological grade) properly adjusted to have the final composition: 10 mM phosphate, 100 mM NaCl, pH 7.4 (HACH GLP Sension+ PH31 pHmeter). Stock solutions in DMSO with a concentration between 1.31×10^{-3} M and 9.1×10^{-4} M were prepared for all the six compounds tested. The samples concentration was adjusted to have an absorbance between 0.1 and 1 at the Abs_{max} to evaluate the general photophysical properties in organic solvents (molar extinction coefficient, Abs_{max}, Em_{max}, Stokes Shift). The photophysical values reported reflect the average over three independent measurements. All the photophysical measurements were carried out in a 1 cm four-sided quartz cuvette from Hellma Analitics. Absorption spectra were measured on a Shimadzu UV-1900i UV-Vis Spectrophotometer, using a resolution of 0.5 nm. Steady state emission and excitation spectra were measured on a Shimadzu RF- 6000. The excitation and the emission slits were set at 5 and 10 nm respectively, while the resolution at 1 nm.

The sample concentrations were adjusted to have an absorbance lower than 0.1 at the excitation wavelength (λ_{ex}) using the above-described stock solutions for all the compounds tested. The fluorescence quantum yields (QY) were evaluated compared to Rhodamine 6G (QY= 0.94 in EtOH, λ_{ex} 500 nm) as external standard by applying the following Equation (1): [43]

$$QY = QY_{STD}\,\frac{I}{I_{STD}}\,\frac{Abs_{STD}}{Abs}\,\frac{n^2}{n_{STD}^2} \quad (1)$$

Where QY_{STD} is the fluorescence quantum yield of the standard, I and I_{STD} are the integrated area of the emission band of the sample and the standard respectively. Abs and Abs_{STD} are the absorbance at the excitation wavelength for the sample and the standard respectively. n and n_{STD} are the solvent refractive indexes of the sample and the standard solutions respectively.

Investigation in Large Unilamellar Vesicles (LUVs)

1,2-Dioleoyl-*sn*-glycero-3-phosphocholine (DOPC) and 1,2-dipalmitoyl-*sn*-glycero-3-phosphocholine (DPPC), Cholesterol (ovine) were purchased from Avanti Polar Lipids.

DOPC LUVs preparation

Thin lipid films were prepared by a slow rotary evaporation (30 °C) of a DOPC (25.0 mg, 0.03 mmol) solution in MeOH/$CHCl_3$ 1:1 (2.0 mL), followed by a final draining (5 h) in vacuo. Each film was hydrated with 1.0 mL buffer (10 mM phosphate, 100 mM NaCl, pH 7.4) for 30 min at rt, subjected to freeze-melt cycles (7×, liquid N_2, 40 °C water bath) and extrusions (17×) through a polycarbonate membrane (pore size, 100 nm) at rt using an Avanti Polar Lipid Mini-Extruder. Final conditions: ~32 mM DOPC; 10 mM phosphate, 100 mM NaCl, pH 7.4. The vesicles were used within 7 days of extrusion and stored in fridge.

DPPC LUVs synthesis

Thin lipid films were prepared by a slow rotary evaporation (50 °C) of a DPPC (22.5 mg, 0.03 mmol) solution in MeOH/$CHCl_3$ 1:1 (2.0 mL), followed by a final draining (5 h) in vacuo. Each film was hydrated with 1.0 mL buffer (10 mM phosphate, 100 mM NaCl, pH 7.4) for 30 min at 55 °C, subjected to freeze-melt cycles (7×, liquid N_2, 55 °C water bath) and extrusions (21×) through a polycarbonate membrane (pore size, 100 nm) at 55 °C using an Avanti Polar Lipid Mini-Extruder. Final conditions: ~31 mM DPPC; 10 mM phosphate,

Organic & Biomolecular Chemistry Accepted Manuscript

100 mM NaCl, pH 7.4. The vesicles were used within 7 days of extrusion and stored in fridge.

DPPC/CL LUVs synthesis

Thin lipid films were prepared by a slow rotary evaporation (50 °C) of a solution of 17 mg DPPC and 4.5 mg CL in MeOH/$CHCl_3$ 1:1 (2.0 mL), followed by a final draining (5 h) in vacuo. Each film was hydrated with 1.0 mL buffer (10 mM phosphate, 100 mM NaCl, pH 7.4) for 30 min at 55 °C, subjected to freeze-melt cycles (7×, liquid N_2, 55 °C water bath) and extrusions (15×) through a polycarbonate membrane (pore size, 100 nm) at 55 °C using an Avanti Polar Lipid Mini-Extruder. Final conditions: ~23 mM DPPC; ~11 mM CL (~34 mM total lipid) 10 mM phosphate, 100 mM NaCl, pH 7.4. The vesicles were within 7 days of extrusion and stored in fridge.

Time dependence analyses (DOPC, DPPC, DPPC/CL)

In a typical procedure, to a 2900 μL buffer (10 mM phosphate, 100 mM NaCl, pH 7.4) in a quartz cuvette, DOPC LUVs (100 μL, 1.1 mM DOPC final), DPPC LUVs (100 μL, 1.02 mM DPPC final) or DPPC/CL LUVs (100 μL, 0.77 mM DPPC final, 0.37 mM CL final) all the six tested compounds (3 μL, of the previously described DMSO stock solutions, ~0.91-1.31 μM final) were added in separated experiments. Each solution was mixed at room temperature and monitored acquiring the emission spectra (λ_{exc} = 470 nm) every 60 s for 15 min. The emission spectra in LUVs of each compound were corrected by the corresponding excitation spectra. Excitation spectra were measured using λ_{em} = 540 nm.

Partition coefficients in DOPC liposomes

In a typical procedure, different DOPC LUVs (32 mM) aliquots were added to a solution of probes **1-6** (3 μL, of the previously described DMSO stock solutions, ~0.91-1.31 μM final in 2900 μL of buffer 10 mM phosphate, 100 mM NaCl, pH 7.4). The fluorescence spectra were recorded at equilibrium after addition of lipids (15 minutes for all the vesicles) The excitation and the emission slits were set at 5 and 5 nm respectively, while the resolution at 1 nm. Then, the maximum intensity (F) was plotted against the lipid concentration (L) for each prepared solution, according to Equation (2):[44]

$$F = \frac{F_0 L}{\frac{55.6}{K_{rip}} + L} \quad (2)$$

where F_0 is the maximum fluorescence resulting from the total probe incorporation into membrane and K_{rip} is the partition coefficient. The double reciprocal plot of the fluorescence (F) and the lipid concentration (L) should give a linear fit, according to Equation (3):

$$\frac{1}{F} = \left(\frac{55.6}{K_{rip}\, F_0}\right) \frac{1}{L} + \frac{1}{F_0} \quad (3)$$

Finally, K_{rip} can be calculated from the slope of the linear fit reported in equation (2), using the F_0 value calculated from the intercept of the fit.

DPPC Liposome phase variation assay (DOPC, DPPC)

In a typical procedure, to a 2900 μL of thermostated buffer (10 mM phosphate, 100 mM NaCl, pH 7.4). in a glass cuvette, DOPC LUVs (100 μl) and probes **1-6** (3 μL, of the previously described DMSO stock solutions, ~0.91-1.31 μM final) were added. The solution was stirred at room temperature for 30 minutes before the spectra acquisition. The temperature was then raised to 55 °C and the solution was kept at this temperature for 30 minutes before the spectra acquisition. Then the temperature lowered down to 25 °C and the spectra were acquired after 30 minutes. The temperature cycle was repeated a second time. The same procedure was applied for DPPC LUVs (100 μL).

DLS

In a typical procedure, to a 3000 μL of buffer (10 mM phosphate, 100 mM NaCl, pH 7.4) in a plastic cuvette, probes **1-6** (3 μL, of the previously described DMSO stock solutions, ~0.91-1.31 μM final) were added. After an equilibration time of 120 s the solutions were measured at 25 °C, using a measurement angle of 173° and a light source wavelength of 632.8 nm. The reported results are the average of six independent measurements per dye.

Cell Culture and Treatments

A549 human lung carcinoma cells (ATCC) were maintained in RPMI Medium 1640 + GlutaMAX (Gibco, Thermo Fisher Scientific), supplemented with 10% fetal bovine serum (FBS, Gibco, Thermo Fisher Scientific,) and 1% penicillin-streptomycin (Gibco, Thermo Fisher Scientific) at 37 °C in a humidified atmosphere with 5% CO_2. The cells were seeded onto sterilized coverslips placed in the wells of a 24-well plate and cultured overnight until reaching 70%–80% confluence. A549 cells were then treated with probes **5** and **6** at the concentration of 10 μM diluted in serum-free RPMI for 30 minutes. The cells were then fixed with 4% paraformaldehyde (PFA) for 15 min at room temperature, following fixation, coverslips were washed three times with PBS. Immunofluorescent counterstaining was performed by staining actin filaments with DyLight 594 Phalloidin (1:300 dilution in 0.1% TritonX) for 15 min at room temperature. Pictures were acquired with a confocal microscope (Leica TCS-II SP8), at 63X magnification.

Results and Discussion

Synthesis

Six 8-aryl-1,3,5,7-tetramethyl BODIPY derivatives, alkoxylated at the aromatic ring at the *para*-position, were designed and synthesized following known literature procedures.[24,28] The simplest dye of the series, the *meso*-(4-methoxyphenyl)-substituted BODIPY **1**, was prepared through the condensation of commercially available *p*-anisaldehyde with 2,4-dimethylpyrrole (2 eq.) in dichloromethane (DCM) in presence of a catalytic amount of trifluoroacetic acid (TFA), followed by oxidation with 2,3-dichloro-5,6-dicyano-1,4-benzoquinone (DDQ) and chelation with $BF_3{\cdot}OEt_2$ in presence of *N*,*N*-diisopropylethylamine (DIPEA), as reported in Scheme 1. This multistep, one-pot procedure was performed without isolation of the intermediate dipyrromethene, and the final compound **1** was obtained in 26% yield after purification. Starting from a series of 4-alkoxysubstituted benzaldehydes, the synthesis of

Organic & Biomolecular Chemistry Accepted Manuscript

This journal is © The Royal Society of Chemistry 20xx

Please do not adjust margins

BODIPY dyes **2-6** was accomplished using the same straightforward one-step procedure, which afforded the desired dyes in modest yield (10-28%) upon purification.

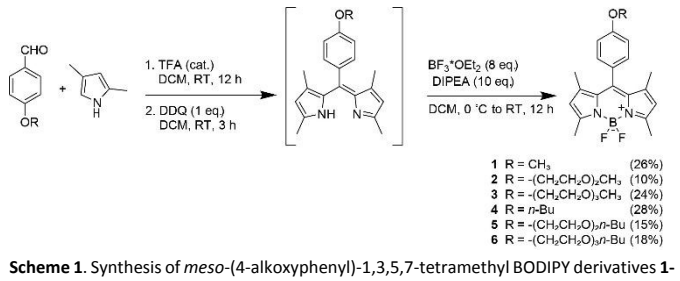

Scheme 1. Synthesis of *meso*-(4-alkoxyphenyl)-1,3,5,7-tetramethyl BODIPY derivatives **1-6**.[24,28]

Photophysical properties

The optical properties of compounds **1-6** were studied in eight different organic solvents and in aqueous buffer solution (pH 7.4) to evaluate the photophysical properties of the dyes in different polar environments (Figures 1 and S1, Tables 1 and S1) before the investigation in LUVs. The compounds present good solubility and no indication of PEG-induced aggregation phenomena in apolar media as toluene and in all the other solvents of different polarity. The absorption spectra were characterized by the typical fingerprint of *meso*-substituted BODIPY with an intense sharp peak in the 498-504 nm region, corresponding to the 0–0 vibrational band of the $S_0 \rightarrow S_1$ transition, which was slightly red-shifted in apolar solvents.[45,46] The characteristic BODIPY shoulder related to the 0-1 vibrational band of the same $S_0 \rightarrow S_1$ transition was also well-defined at higher energies in the 465-475 nm region of the spectra. Compounds **1-6** displayed a remarkable chromophore character in all solvents, characterized by comparable average molar extinction coefficient (ε) of 104000, 113000, 112000 and 115000 $M^{-1}cm^{-1}$ for probes **1-4**, respectively, and lower values of 87500 and 87400 $M^{-1}cm^{-1}$ for BODIPYs **5** and **6**. Similar trend was also observed for the emission spectra located in the 508-515 nm region of the spectra for all the compounds in different media. Minimal bathochromic shift of the emission maxima was recorded in apolar solvents in comparison to polar environments. As expected, due to the symmetrical structure of the dyes, no remarkable solvatochromic behaviour was recorded with an almost constant averaged value of 11 nm for the Stokes shifts in solvents.[47,48] High values of fluorescence quantum yield were recorded for **1-6** ranging from 0.70 in apolar media to 0.50 in polar solvents such as methanol and acetonitrile. All six compounds were characterized by similar variations of emission intensities as a function of solvent polarity. Different photophysical behaviour of BODIPYs **1-6** were observed in aqueous buffer solution at pH 7.4 where the length and type of the alkyl terminal of the ethylene glycol moieties played a key role. In the **1-3** series, characterized by a methyl group on terminal oxygen atom at the *meso* position, compounds **2-3** provided well-defined absorption and emission peaks resembling the data recorded in organic solvents, while BODIPY **1** was characterized by a larger and lower peak in absorption and much less intense signal in emission in comparison to the spectra in other media.

A more careful look at the photophysical data revealed a drop of 61%, 44% and 15% in the molar extinction coefficients for compounds **1-3**, respectively, which is reasonably indicative either of dye precipitation or of the formation of aggregates. It is reasonable to speculate that the MeO group in **1** is not hydrophilic enough to confer complete solubilization of the probe in buffer which therefore tends to form aggregates characterized by a significant drop of the fluorescence quantum yield. The elongation of the hydrophilic chain of one ethylene glycol unit in **2** provides much higher compatibility with water, thus limiting the aggregates formation. These results were clearly depicted by a typical BODIPY shape in the absorption and emission spectra, a comparable value of the fluorescence quantum yield to the ones calculated in organic media, while the ε was still affected by a drop of 44% suggesting the formation of soluble aggregates. Further insertion of another ethylene glycol unit in **3** almost completely restored the molecular features recorded in different organic solvents. The molar extinction coefficient of **3** in buffer was comparable to the values recorded in THF and MeOH while the fluorescence quantum yield was even higher than in apolar media, strongly suggesting an almost complete solubilization of the dye in water. The replacement of the terminal methyl with a *n*-butyl group almost completely hampered the solubilization of compounds **4-6** in water due to the higher hydrophobic character of the probes. In the three molecules of the series the absorption spectra were remarkably affected by aggregation with a drop of the molar extinction coefficients of 68%, 65% and 63% respectively for **4**, **5** and **6** neutralizing the solubilization effect related to the ethylene glycol moieties. Similarly, the QY of the dyes were strongly quenched from around 0.70 to 0.15, 0.09 and 0.12 values, highlighting the dominant effect on solubility of the terminal group of the ethylene glycol chain with respect to the chain length.

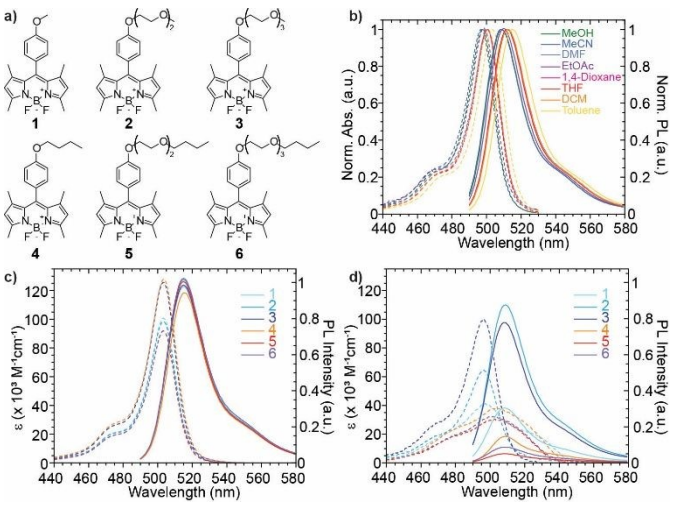

Figure 1. a) Molecular structures of the BODIPY-based probes **1-6**; b) Absorption (dashed) and emission (solid) spectra of **1** in different solvents; c) Absorption (dashed) and emission (solid) spectra of **1-6** in toluene; d) Absorption (dashed) and emission (solid) spectra of **1-6** in phosphate buffer solution (pH 7.4).

Dynamic Light Scattering (DLS) measurements were performed in buffer solution of dye **1-6** to further investigate the formation and presence of dyes aggregates in aqueous media (Figure S2). The experimental results for **4-6** confirmed the presence of comparable size aggregates of **4** and **6** with a 110.7±5 nm and 114.1±8 nm diameter respectively, while **5** was characterized by slightly large aggregates with diameters around 126.2±10 nm. On the other hand,

Organic & Biomolecular Chemistry Accepted Manuscript

no clear evidence was observed for the formation of aggregates in water for **1-3**. Minimal kcps values were recorded for **2** and **3** confirming the water solubilizing effects of the ethylene glycol subunits and the minimal hydrophobic effect of the OMe terminal, while dye **1** was characterized by high value of kcps but no experimental evidence of aggregates presence.

Table 1. Photophysical parameters of compounds **1-6** in toluene.

	λ_{abs}[a]	ε[a]	λ_{em}[a]	QY[b]	Brightness[a]	Stokes shift[a]
1	504	101498±6	515	0.69±0.02	70033	11
2	504	99435±16	515	0.72±0.03	71593	11
3	504	127163±25	515	0.68±0.01	86471	11
4	504	128802±17	515	0.73±0.01	94025	11
5	504	92413±21	515	0.73±0.02	68775	11
6	504	92775±11	515	0.74±0.02	68654	11

[a] λ_{abs}, λ_{em} are reported in nm. ε, Brightness and Stokes shift are reported in $M^{-1}cm^{-1}$, in $M^{-1}cm^{-1}$ and nm, respectively. [b] QY was measured referring to Rhodamine 6G as standard.

Studies in LUVs membranes

Compounds **1-6** were investigated as intercalating fluorophores for membrane bioimaging aiming at analysing the impact of the structural differences in terms of *para*- substituents variation on the *meso* phenyl moiety. The studies were performed by using LUVs of 1,2-dioleoyl-*sn*-glycero-3-phosphocholine (DOPC), 1,2-dipalmitoyl-*sn*-glycero-3-phosphocholine (DPPC) and a mixture of DPPC and cholesterol (CL) to simulate respectively lipid liquid disorder, solid ordered and liquid ordered phases at room temperature. The interaction between the bilayer membranes and the probes was monitored by steady-state fluorescence measurements (Figures 2 and S3-S9). All the probes, except compounds **2** and **3**, were characterized by a partially quenched emission in buffer, which resulted particularly significant for dyes **5** and **6** as already observed in the photophysical assays. The interaction with the hydrophobic liposome bilayer was depicted by an emission turn-on for all the compounds with a general emission maximum red-shifted upon intercalation. In the series of probes **1-3**, bearing a methoxy group as terminal unit of the *meso* group, the fluorescence response was comparable among the three scaffolds and the different lipid phases with a slightly higher intensity in highly packed DPPC LUVs which could be directly related to the higher QY values in more apolar environments. The presence of the ethylene glycol moieties already conferred good solubility to **2** and **3** in buffer solution and the subsequent intercalation into the lipid bilayer was depicted by hyper and bathochromic shifts of the emission spectra suggesting the localization of the probes in the medium polarity region of the membrane leaflet in agreement with the emission signal recorded in THF and 1,4-dioxane. Compound **2** showed an overall higher fluorescence response, but lower discrimination of the membrane phases compared to the analogue with longer ethylene glycol **3**. It is worth noting how the addition of a single ethylene glycol units on the molecular scaffold of **2** can affect the probe interactions with the lipid bilayer, providing for compound **3** a different response pattern despite the similar photophysical features between **2** and **3**. Nevertheless, neither **2** or **3** would be an ideal candidate for membrane imaging because of the comparable emission intensity of the probes is buffer media.

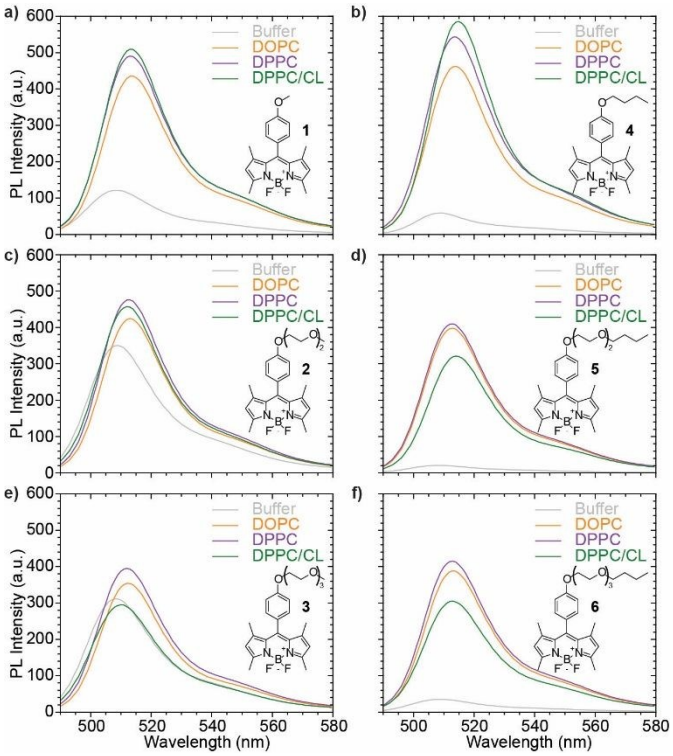

Figure 2. Emission spectra of probes a) **1**, b) **4**, c) **2**, d) **5**, e) **3** and f) **6** in buffer (gray), DOPC (orange), DPPC (purple) and DPPC/CL (green) LUVs after 15 min of equilibration time.

On the other hand, the emission of **1** was strongly quenched in buffer most likely due to aggregates formation, as previously discussed in the photophysical section. The addition of LUVs to the buffer solution of **1** promoted the disaggregation/partition of the dye inside the membrane bilayer described by a 4-5 times increase of the emission signal in all three liposomal systems. The replacement of the terminal methyl unit with a *n*-butyl moiety drastically affected the photophysical properties of compounds **4-6** in buffer promoting the formation of self-quenched aggregates of the BODIPY-based probes. These three dyes behaved as fluorogenic membrane probes capable of lighting up in presence of membrane bilayer. As for the **1-3** series, the bilayer membrane phase discrimination with compounds **4-6** was possible with a remarkable turn-on of the emission intensities upon intercalation. Interestingly, the turn on values of compounds **4** and **6** were much similar than with **5** confirming that small side functionalization on fluorophores, not even directly related to π system dimension and/or electron delocalization, can clearly affect the final application in imaging in terms of signal to noise ratio or selectivity. The higher hydrophobic character of **4** compared to **1** improved the affinity to less polar systems like DPPC and DPPC-cholesterol over the more hydrated DOPC membranes. Comparable responses to **3** was recorded for **6** indicating that the extended ethylene glycol chain played a key role in addressing the interactions with the different membrane bilayer phases and the probe more than the terminal alkyl residue. The intercalation results of **5**, instead,

Organic & Biomolecular Chemistry Accepted Manuscript

This journal is © The Royal Society of Chemistry 20xx

Please do not adjust margins

were remarkably different to what observed for the analogue **2**. While the interaction with the more hydrated and flexible DOPC was comparable between **2** and **5**, the elongation of the alkyl chain partially hampered the incorporation in the more rigid DPPC and DPPC-cholesterol probably due to a higher steric hindrance. In terms of membrane discrimination, the best results were observed for the small hydrophobic **4** while the higher turn-on values up to twenty times in intensity were recorded for the mono ethylene glycol decorated **5** (Table S2). Due to the small, yet detectable, variation in emission intensities recorded in different liposome systems, dye **1-6** were tested in DPPC phase-transition temperature to evaluate the emission response to environment change. DPPC membranes are well-known for solid ordered gel to fluid liquid disordered phase transition occurring at 41 °C.[49] DPPC and DOPC liposomes stained with **1-6** were subjected to heating at 55 °C and cooling cycles at 25 °C to record the emission response of the BODIPY probes. Similar trend was observed for both liposome systems (Figure S10 and S11) showing a significant decrease of the emission signals at 55 °C and a subsequent recovery of the signal upon cooling down the solution at room temperature. The trend similarity recorded for all probes in both DPPC and DOPC, as negative control, systems strongly indicated a predominant effect on the probes QY of the temperature, promoting the non-radiative pathways for the energy decay, rather than the effect of different nature of the membrane phase in DPPC. Nevertheless, upon re-equilibration at 25 °C the original emission intensities of all dyes **1-6** were recorded, suggesting stable partition of the probes within the membranes.

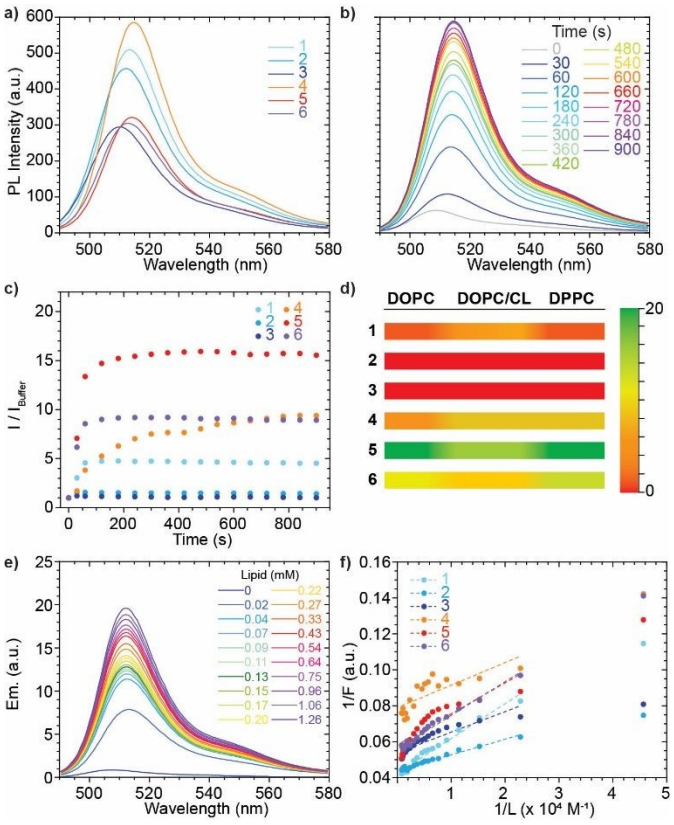

Figure 3. a) Emission spectra of probes **1-6** DPPC/CL LUVs after 15 mins of equilibration time; b) Emission spectra of **4** over time upon addition of DPPC/CL LUVs; c) Emission intensity over time for probes **1-6** with DPPC/CL LUVs; d) Graphical representation of the emission turn-on for probes **1-6** upon intercalation in LUVs; e) Emission spectra of **5** at increasing DOPC liposome concentrations; f) Double reciprocal plot of emission intensity (F) versus DOPC liposome concentration (L) for probes **1-6**.

The experimental traces in the partition kinetics highlighted similar trends of probes **1-6** in the three different liposome systems independently of the membrane fluidity. All the fluorophores were characterized by an increase of the emission intensity and a detectable bathochromic shift, due to the interaction with a more hydrophobic environment, from the spectra recorded in buffer (Figures 3a-d and S9). BODIPY **1** showed a five-fold light up by interacting with the membrane bilayers, reaching an emission plateau in around 200 s. The ethylene glycol extension in **2** and **3**, conferring more pronounced amphiphilic character to the probes, shortened the partition time into the membranes to around 100 and 50 seconds respectively. Nevertheless, the lower degree of aggregation in buffer of **2** and **3** restored a good emission intensity already in buffer which is not ideal in bioimaging applications giving rise to high background noise. The larger hydrophobic character of the terminal butyl moieties in **4-6** had a remarkable effect on the partition process. The high hydrophobic character of **4** induced aggregation in buffer switching off almost completely the emission. The membrane intercalation process was therefore depicted by a ten folds increase of the emission intensity upon interaction with LUVs to reach a plateau at around 400 seconds, almost twice the time required by the analogue **1**. Similarly to the first series, the elongation of the ethylene glycol units cut the partition equilibria time to 200 and 100 s respectively in dyes **5** and **6**. The replacement of the terminal methyl unit with longer *n*-butyl alky chain conferred good emission light up of the probes upon interaction with the amphiphilic membranes and also provided better discrimination of the membrane phases. In parallel the affinity of the BODIPY probes towards the hydrophobic membrane was explored by evaluating the partition coefficients of **1-6** between water and DOPC membrane (Figure 3e and S12). All six probes were characterized by partition coefficient values in the range from 1.21 x 10^6 of **1** to 3.51 x 10^6 of **4** which are comparable to other membrane probes reported in literature.[9,44] The different length of the ethylene oxide moieties, as well as the terminal alkyl chain have no remarkable effect of the partition coefficient of the dyes suggesting that the BODIPY core plays a key role in the partition process. The addition of one or two ethylene glycol units in **2** and **3** doubles the partition coefficient to 2.82 and 2.63 x 10^6 respectively. Opposite trend is observed in the butyl series **4-6** where the addition of one or two ethylene oxide reduced the partition coefficients to 1.87 x 10^6 in **5** and 1.66 x 10^6 in **6**. Nevertheless, in the double reciprocal plot (Figure 3f), the linear fit for dyes **4** and **5** were affected by clear deviation from linearity, suggesting the presence of concurrent and comparable equilibria other than the partition between the buffer phase and membrane bilayer.[50,51] It is reasonable to speculate that these phenomena involve either probe's solubilization and diffusion equilibria or the presence of aggregates in buffer which interact with the liposome membranes. All six probes were potentially suitable for further investigation in cells. Among them **5** and **6** were selected as optimal candidates for bioimaging investigation considering their quick partition kinetics, good partition coefficient into membrane bilayer and, most importantly, the emission turn on upon interaction with liposome membranes.

Organic & Biomolecular Chemistry Accepted Manuscript

Cell Imaging

Among the six reported probes, **5** and **6,** characterized by the higher turn on values which suggest a negligible background fluorescence, were selected to perform immunofluorescence imaging. A549 human lung carcinoma cells (ATCC) were treated with 10 μM diluted in serum-free RPMI for 30 minutes prior to the image acquisition. Confocal microscopy analysis revealed a distinct and compartmentalized internalization of **5** and **6** within the cellular cytoplasm (Figure 4).

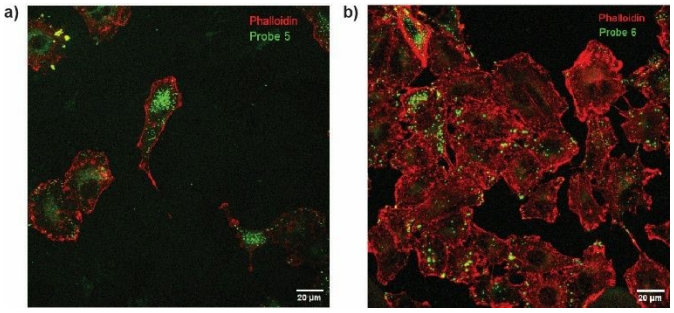

Figure 4. A549 lung cancer cells incubated with a) **5** and b) **6** at 10 μM concentration with DyLight 594 Phalloidin for actin filaments staining.

The probes exhibit a highly punctate staining pattern, strongly suggesting selective accumulation within vesicular compartments. Co-staining with phalloidin for filamentous actin (F-actin) clearly delineates the cellular morphology and boundaries, confirming that both probes effectively penetrate the plasma membrane without showing direct colocalization with the cytoskeletal structures. Furthermore, a moderate heterogeneity is observed among adjacent cells, which display varying vesicular distribution patterns and signal intensities, although without evident morphological alterations indicative of acute toxicity. These preliminary results confirmed that the amphiphilic character of **5** and **6** allowed interesting bioimaging outputs.

Conclusion

The small library of differently substituted BODIPYs synthesized in this work has highlighted once more the interesting properties of BODIPY dyes in chemical biology. Straightforward synthesis and good structural variety have allowed to obtain in a single step and with moderate yields the complete library of BODIPYs. The systematic variation on the length and terminal of the ethylene glycol moieties allowed the rationalization on how even small modifications on the molecular edges can play a crucial role in tuning the final probes features towards specific targets. PEGylation of synthetic probes has been widely used over the years to protect them, improve their solubility or the transfection efficiency in chemical biology applications. Here we have highlighted, starting from well-known probes like BODIPY, how PEGylation should also be properly designed according to the final application since the length and type of ethylene glycol moiety can have remarkable positive or negative effect on the probes. This BODIPYs' library has been designed to get deep insight on how minimal structural variations and straightforward synthetic accessibility can affect the visualization of amphiphilic biological compartments with small and compact dyes. The probes herein reported are not aimed to compare with commercially available probes nor to overcome parent dye well-designed in combination with biomolecules as DPPC, PC and cholesterol or more complex molecular structures.[52–57] Instead a minimalistic approach is here reported to highlight how minimal structural modification can confer or hamper the feature and functionality of final probes. The results reported by varying the hydrophilic/hydrophobic character of a well-known dye allows to optimize the emissive read-outs in relationship to the molecular structures. This approach is essential to find an appropriate balance between many key features in bioimaging applications such as solubility, specificity and signal to noise ratio, providing fundamental and basic information for the design of novel bioimaging tools for biochemical oriented purposes.

Author contributions

Martina Fresia: formal analysis (equal); investigation (supporting). Francesco Marra: formal analysis (equal); investigation (equal). Giacomo Renno: formal analysis (equal); investigation (lead); data curation (equal); writing—review & editing (supporting). Giada Fregnan: formal analysis (equal); data curation (equal). Davide Zanetti: formal analysis (equal); investigation (supporting). Federica Micheletto: formal analysis (equal); investigation (equal). Paolo Ettore Porporato: supervision (equal); writing—review & editing (equal). Francesca Cardano: data curation (lead); formal analysis (equal); supervision (supporting); validation (lead); writing—original draft (lead); writing—review & editing (equal). Marco Blangetti: conceptualization (lead); funding acquisition (lead); supervision (equal); writing—original draft (lead); writing—review & editing (equal). Andrea Fin: conceptualization (lead); data curation (lead); funding acquisition (lead); supervision (equal); writing—original draft (lead); writing—review & editing (equal).

Conflicts of interest

The authors declare no conflict of interest.

Data availability

The data underlying this study are available in the published article and its SI: general procedures, experimental details, characterization data for both new and known compounds, copies of ^{1}H, ^{13}C spectra, photophysical data, absorption and emission spectra, partition kinetic emission traces, are provided in the SI (PDF). See DOI:

Acknowledgements

Organic & Biomolecular Chemistry Accepted Manuscript

This journal is © The Royal Society of Chemistry 20xx

Please do not adjust margins

The authors acknowledge support from the project CH4.0 under the MUR program "Dipartimenti di Eccellenza 2023–2027" (CUP: D13C22003520001).

Notes and references

1 L. D. Lavis and R. T. Raines, *ACS Chem. Biol.,* 2014, **9**, 855–866.
2 F. de Moliner, F. Nadal-Bufi, M. Vendrell, *Curr. Opin. Chem. Biol.*, 2024, **80**, 102458.
3 C. Dias, J. Nylandsted, *Cell Discov.*, 2021, **7**, 1–18.
4 J. V. Jun, D. M. Chenoweth, E. J. Petersson, *Org. Biomol. Chem*., 2020, **18**, 5747–5763.
5 K. Li, S. Xu, M. Xiong, S. Y. Huan, L. Yuan, X. B. Zhang, *Chem. Soc. Rev.,* 2021, **50**, 11766–11784.
6 X. Cheng, J. C. Smith, *Chem. Rev.*, 2019, **119**, 5849–5880.
7 G. L. Nicolson, *BBA-Biomembranes*, 2014, **1838**, 1451–1466.
8 M. Collot, S. Pfister, A. S. Klymchenko, *Curr. Opin. Chem. Biol.*, 2022, **69**, 102161.
9 G. Renno, F. Cardano, V. Ilieva, G. Viscardi, A. Fin, Eur. *J. Org. Chem.*, 2022, e202200833.
10 F. Cardano, F. Micheletto, G. Fregnan, G. Renno, P. E. Porporato, A. Fin. *Eur. J. Org. Chem.*, 2025, e202500363.
11 M. Collot, P. Ashokkumar, H. Anton, E. Boutant, O. Faklaris, T. Galli, Y. Mély, L. Danglot, A. S. Klymchenko, *Cell Chem. Biol.*, 2019, **26**, 600–614.
12 D. Alonso Doval, A. Fin, M. Takahashi-Umebayashi, H. Riezman, A. Roux, N.Sakai, S. Matile *Org. Biomol. Chem.*, 2012,**10**, 6087-6093
13 G. Renno, F. Cardano, G. Volpi, C. Barolo, G. Viscardi, A. Fin, *Molecules*, 2022, **27**, 3856.
14 D. I. Danylchuk, P. H. Jouard, A. S. Klymchenko, *J. Am. Chem. Soc.*, 2021, **143**, 912–924.
15 A. S. Klymchenko, *Acc. Chem. Res.*, 2022, **56**, 1–12.
16 J. Ma, R. Sun, K. Xia, Q. Xia, Y. Liu, X. Zhang, *Chem. Rev.*, 2024, **124**, 1738–1861.
17 M. Dal Molin, Q. Verolet, A. Colom, R. Letrun, E. Derivery, M. Gonzalez- Gaitan, E. Vauthey, A. Roux, N. Sakai, S. Matile, *J. Am. Chem. Soc.*, 2015, **137**, 568–571.
18 N. Aknine, R. Pelletier, A. S. Klymchenko, *JACS Au*, 2025, **5**, 922–936.
19 R. Ziessel, G. Ulrich, A. Harriman, *New J. Chem.*, 2007, **31**, 496–501.
20 H. B. Cheng, X. Cao, S. Zhang, K. Zhang, Y. Cheng, J. Wang, J. Zhao, L. Zhou, X. J. Liang, *Adv. Mater.*, 2023, **35**, 2207546.
21 Z. Mao, J. H. Kim, J. Lee, H. Xiong, F. Zhang, J. S. Kim, Coord. *Chem. Rev.*, 2023, **476**, 214908.
22 A. Treibs, F. H. Kreuzer, *Justus Liebigs Ann. Chem.*, 1968, **718**, 208–223.
23 P. Lu, K. Y. Chung, A. Stafford, M. Kiker, K. Kafle, Z.A. Page, *Polym. Chem.*, 2021, **12**, 327–348.
24 C. Bellomo, D. Zanetti, F. Cardano, S. Sinha, M. Chaari, A. Fin, A. Maranzana, R. Núñez, M. Blangetti, C. Prandi, *Dyes Pigm.*, 2021, **194**, 109644.
25 X. Hu, Z. Fang, C. Zhu, Y. Yang, Z. Yang, W. Huang, *Adv. Funct. Mater.*, 2024, **34**, 2401325.
26 W. Qin, M. Baruah, M. Van der Auweraer, F. C. De Schryver, N. Boens, *J. Phys. Chem. A*, 2005, **109**, 7371–7384.
27 A. Loudet, K. Burgess, *Chem. Rev.*, 2007, **107**, 4891–4932.
28 G. Ulrich, R. Ziessel, A. Harriman, *Angew. Chem. Int. Ed.*, 2008, **47**, 1184–1201.
29 S. Adhikari, J. Moscatelli, E. M. Smith, C. Banerjee, E. M. Puchner, *Nat. Commun.*, 2019, **10**, 3400.
30 S. Wang, L. Gai, Y. Chen, X. Ji, H. Lu, Z. Guo, *Chem. Soc. Rev.*, 2024, **53**, 3976–4019.
31 W. J. Shi, X. H. Yan, J. Yang, Y. F. Wei, Y. T. Huo, C. L. Su, J. Yan, D. Han, L. Niu, *Anal. Chem.*, 2023, **95**, 9646–9653.
32 P. Kaur, K. Singh, *J. Mat. Chem. C*, 2019, **7**, 11361–11405.
33 Y. Zhang, K. Song, S. Tang, L. Ravelo, J. Cusido, C. Sun, H. F. Zhang, F. M. Raymo, *J. Am. Chem. Soc.*, 2018, **140**, 12741–12745.
34 M. Páez-Pérez, M. K. Kuimova, *Angew. Chem. Int. Ed.*, 2024, **63**, e202311233.
35 M. Páez-Pérez, I. López-Duarte, A. Vyšniauskas, N. J. Brooks, M. K. Kuimova, *Chem. Sci.*, 2021, **12**, 2604–2613.
36 G. Rotas, M. B. Thomas, R. Canton-Vitoria, F. D'Souza, N. Tagmatarchis, *Chem. Eur. J.*, 2020, **26**, 6652–6661.
37 S. Erbas-Cakmak, E.U. Akkaya, *Angew. Chem. Int. Ed.*, 2013, **125**, 11574–11578.
38 M. S. Wong, M. Samoc, A. Samoc, B. Luther-Davies, M. G. Humphrey, *J. Mat. Chem.*, 1998, **8**, 2005–2009.
39 S. Pisano, D. Milano, N. Passoni, E. Iengo, P. Tecilla, *J. Porphyr. Phthalocyanines*, 2016, **20**, 514–524.
40 J. Ma, F. Luo, C. H. Hsiung, J. Dai, Z. Tan, S. Ye, L. Ding, B. Shen, X. Zhang, *Angew. Chem. Int. Ed.*, 2024, **63**, e202403029.
41 X. Yi, J. Zhao, J. Sun, S. Guo, H. Zhang, *Dalton Trans.*, 2013, **42**, 2062–2074.
42 L. X. Gao, M. Tian, L. Zhang, Y. Liu, F. L. Jiang, *Dyes Pigm.*, 2020, **180**, 108434.
43 A. M. Brouwer, *Pure Appl. Chem.*, 2011, **83**, 2213–2228.
44 Z. Huang, R. P. Haugland, *Biochem. Biophys. Res. Commun.*,1991, **181**, 166-171.
45 A. Filarowski, M. Kluba, K. Ciéslik-Boczula, A. Koll, A. Kochel, L. Pandey, W. M. De Borggraeve, M. Van der Auweraer, J. Catalànc, N. Boens, *Photochem. Photobiol. Sci.*, 2010, **9**, 996–1008.
46 N. A. Bumagina, E. V. Antina, A. A. Ksenofontov, L. A. Antina, A. A. Kalyagin, M. B. Berezin, *Coord. Chem. Rev.*, 2022, **469**, 214684.
47 L. Cunha Dias de Rezende, M. Menezes Vaidergorn, J. C. Biazzotto Moraes, F. da Silva Emery, *J. Fluoresc.*, 2014, **24**, 257–266.
48 C. Reichardt, *Angew. Chem. Int. Ed.*, 1979, **18**, 98–110.
49 R. Koynova, M. Caffrey, *Biochim. Biophys. Acta* 1998, **1376**, 91–145.
50 V.N. Uversky, P.P. Madeira, B.Y. Zaslavsky, *Int. J. Mol. Sci.,* 2024, **25**, 6339–6364.
51 E. Fritschka, G. Sadowski, *Mol. Pharmaceutics*, 2025, **22**, 4930−4939.
52 K. P. Armendariz, H. A. Huckabay, P. W. Livanec, R.C. Dunn, *Analyst,* 2012, **137**, 1402–1408.
53 I. A. Boldyrev, X. Zhai, M. M. Momsen, H. L. Brockman, R. E. Brown, J. G. Molotkovsky, *J. Lipid Res.*, 2007, **48**, 1518–1532.
54 D. L. Marks, R. Bittman, R. E. Pagano, *Histochem. Cell Biol.,* 2008, **130**, 819–832.
55 T. Xiong, Y. Chen, Q. Peng, M. Li, S. Lu, X. Chen, J. Fan, L. Wang, X. Peng, *J. Am. Chem. Soc.,* 2024, **146**, 24158−24166.
56 S. Serrano-Buitrago, M. Muñoz-Úbeda, V. G. Almendro-Vedia, J. Sánchez-Camacho, B. L. Maroto, F. Moreno, J. Bañuelos, I. García-Moreno, I. López-Montero, S. de la Moya; *J. Mater. Chem. B*, 2023; **11**, 2108–2114.
57 M. Collot, E. Boutant, M. Lehmann, A. S. Klymchenko, *Bioconjugate Chem.,* 2019, **30**, 192−199.

Organic & Biomolecular Chemistry Accepted Manuscript

Please do not adjust margins

Dipartimento
Chimica

UNIVERSITÀ
DI TORINO

2023 - 2027
DIPARTIMENTO
DI ECCELLENZA
Ministero dell'Università e della Ricerca

Prof. Andrea Fin
E-mail: andrea.fin@unito.it

Manuscript Title: Structural and photophysical evaluation of O-alkoxy substituted BODIPY dyes in liposomes
Authors: Martina Fresia, Francesco Marra, Giacomo Renno, Davide Zanetti, Federica Micheletto, Francesca Cardano, Marco Blangetti, Andrea Fin

The data underlying this study are available in the published article and its SI: general procedures, experimental details, characterization data for both new and known compounds, copies of ^{1}H, ^{13}C spectra, photophysical data, absorption and emission spectra, partition kinetic emission traces, are provided in the SI.

Andrea Fin

Organic & Biomolecular Chemistry Accepted Manuscript

chimica

Università degli Studi di Torino
Dipartimento di Chimica
Via Pietro Giuria 7 – 10125 Torino (TO)
Tel (011) 670 6692 – 670 3466 | Mail: direzione.chimica@unito.it PEC: chimica@pec.unito.it